

Prediction of the Conditions for Breathing of Metal Organic Framework Materials Using a Combination of X-ray Powder Diffraction, Microcalorimetry, and Molecular Simulation

Philip L. Llewellyn,^{*,†} Guillaume Maurin,[‡] Thomas Devic,[§] Sandra Loera-Serna,[†]
Nilton Rosenbach,[‡] Christian Serre,[§] Sandrine Bourrelly,[†] Patricia Horcajada,[§]
Yaroslav Filinchuk,^{||} and Gérard Férey^{§,⊥}

Laboratoire Chimie Provence, Universités d'Aix-Marseille I, II et III - CNRS,
UMR 6264, Centre de Saint Jérôme, 13397 Marseille, France, Institut C. Gerhardt Montpellier,
UMR CNRS 5253, UM2, ENSCM, Place E. Bataillon, 34095 Montpellier cedex 05, France,
Institut Lavoisier (UMR CNRS 8180), Université de Versailles Saint-Quentin-en-Yvelines, 45
avenue des Etats-Unis, 78035 Versailles cedex, France, SNBL at ESRF,
38043 Grenoble, France, and Institut Universitaire de France, 103, bd Saint-Michel,
75005 Paris, France

Received May 30, 2008; E-mail: Philip.llewellyn@univ-provence.fr

Abstract: The adsorption of C1 to C4 linear hydrocarbons in the flexible metal organic framework MIL-53(Cr) has been followed by adsorption manometry coupled with microcalorimetry and Synchrotron X-ray powder diffraction. This experimental investigation was completed by molecular modeling. In the case of methane, the solid remains rigid whatever the adsorbate amount. However for the C2–C4 series, an increasing flexibility of the structure is observed, which is ascribed first to a breathing of the material from a large pore to a narrow pore form followed by a further expansion at high pressure. The collected thermodynamic and structural information suggests that a minimum adsorption enthalpy of ca. 20 kJ mol⁻¹ in the initial large pore structure of MIL-53(Cr) is required to induce the structural transition “large to narrow pore”. Further, the enthalpy of adsorption can be used to predict the pressure at which the structure reopens. Finally, the magnitude of the breathing can be related to the size of the probe molecule via the van der Waals volume. The above trends have been successfully verified in the case of water and carbon dioxide. This combined experimental and theoretical approach gives the first elements for the prediction of whether or not the MIL53 and similar flexible structures will respond to gas loading and what would be the pressure required and further the amplitude of the induced breathing.

Introduction

Porous metal organic framework materials (MOFs) are currently very topical^{1–3} due to their potential in terms of hydrogen^{4–6} and carbon dioxide^{7–11} storage capacity or in liquid separation¹² and drug delivery.¹³ These exceptional properties arise from the possibility to easily change either their metal center or the organic linker unit. It is thus possible to tune the pore size, shape, and connectivity by subtle modifications of the inorganic and/or the organic moieties. To date, over a thousand structures have been documented which provide a library of ordered structures larger than that of the zeolite family.

One extraordinary property of some of these MOFs is their structural flexibility or ‘breathing’,^{1,2,14–18} which allows them to reversibly modulate their pore size according to the molecules

adsorbed into the pores, including gases^{7,9,19–23} and liquids,²⁴ while maintaining their crystallinity and thus their long-range order. Such solids include the chromium or aluminum terephthalates M(OH)(₂OC-C₆H₄-CO₂)·x(solvent), i.e. MIL-53,²⁵ and

[†] Universités d'Aix-Marseille I, II et III - CNRS.

[‡] Institut C. Gerhardt Montpellier.

[§] Université de Versailles Saint-Quentin-en-Yvelines.

^{||} SNBL at ESRF.

[⊥] Institut Universitaire de France.

(1) Férey, G. *Chem. Soc. Rev.* **2008**, *37* (1), 191–214.

(2) Maji, T. K.; Kitagawa, S. *Pure Appl. Chem.* **2007**, *79* (12), 2155–2177.

(3) Rowsell, J. L. C.; Yaghi, O. M. *Microporous Mesoporous Mater.* **2004**, *73* (1–2), 3–14.

(4) Latroche, M.; Sublé, S.; Serre, C.; Mellot-Draznieks, C.; Llewellyn, P. L.; Lee, J.-H.; Chang, J.-S.; Jhung, S. H.; Férey, G. *Angew. Chem., Int. Ed.* **2006**, *45*, 8227–8231.

(5) Liu, Y.; Eubank, J. F.; Cairns, A. J.; Eckert, J.; Kravtsov, V. C.; Luebke, R.; Eddaoudi, M. *Angew. Chem., Int. Ed.* **2007**, *46*, 3278–3283.

(6) Li, Y.; Yang, R. T. *Langmuir* **2007**, *23*, 12937–12944.

(7) Bourrelly, S.; Llewellyn, P. L.; Serre, C.; Millange, F.; Loiseau, T.; Férey, G. *J. Am. Chem. Soc.* **2005**, *127*, 13519–13521.

(8) Furukawa, H.; Miller, M. A.; Yaghi, O. M. *J. Mater. Chem.* **2007**, *17*, 3197–3204.

(9) Llewellyn, P. L.; Bourrelly, S.; Serre, C.; Vimont, A.; Daturi, M.; Hamon, L.; De Weireld, G.; Chang, J.-S.; Hong, D.-Y.; Hwang, Y. K.; Jhung, S. H.; Férey, G. *Langmuir* **2008**, *24* (14), 7245–7250.

(10) Llewellyn, P. L.; Bourrelly, S.; Serre, C.; Filinchuk, Y.; Férey, G. *Angew. Chem., Int. Ed.* **2006**, *45*, 7751–7754.

(11) Serre, C.; Bourrelly, S.; Vimont, A.; Ramsahye, N. A.; Maurin, G.; Llewellyn, P. L.; Daturi, M.; Filinchuk, Y.; Leynaud, O.; Barnes, P.; Férey, G. *Adv. Mater.* **2007**, *19*, 2246–2251.

(12) Alaerts, L.; Kirshhock, C. E. A.; Maes, M.; van der Veen, M. A.; Finsy, V.; Depla, A.; Martens, J. A.; Baron, G. V.; Jacobs, P. A.; Denayer, J. F. M.; De Vos, D. E. *Angew. Chem., Int. Ed.* **2007**, *46*, 4293–4297.

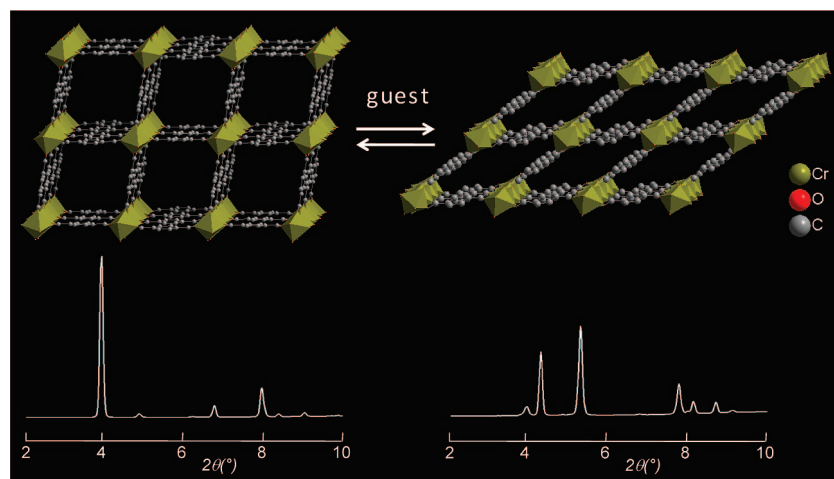


Figure 1. Structures of MIL-53(Cr) in its large pore (top left) and narrow pore (top right) forms (hydrogen atoms omitted). The corresponding X-ray powder diffraction patterns are given below these structures ($\lambda \sim 0.71110 \text{ \AA}$).

the iron/chromium dicarboxylates $M_3OX_2(OC-R-CO_2)_3 \cdot x(\text{sol}v)$, i.e. MIL-88²⁴ (where $X = F, OH, Cl, \text{acetate}, \dots$; $R = \text{fumarate}$ (88A), terephthalate (1,4-BDC) (88B), 2,6-naphthalenedicarboxylate (2,6-NDC) (88C), and 4,4'-biphenyldicarboxylate (4,4'-BPDC) (88D)). They exhibit a reversible expansion/reduction of their cell volume upon sorption/desorption of various species from 40% up to 230%, respectively, and open novel applications of MOFs in addition to current uses of other nanoporous materials.

Two questions arise from this unusual phenomenon: (i) what are the structural characteristics which allow breathing to occur and (ii) as soon as a solid presents these characteristics, what are the thermodynamic conditions for the host–guest interactions which allow the breathing to happen and to what magnitude? For the MIL53(Cr) structure, the first point was recently solved.^{1,11} Besides the necessity of having exclusively even-membered rings in the structure, it highlights the ‘kneecap’ role played by the O–O axis of the carboxylate function during the breathing movement. Concerning the second question, there is still a need for fundamental studies to gain a complete understanding of this phenomenon. While X-ray diffraction reveals the structure of the MOFs and their phase transitions during the adsorption, this tool is not able to answer the fundamental question of why MOF materials are flexible upon the adsorption of some probe molecules and not to others. On the other hand, microcalorimetry can follow the energy profile along the whole adsorption process and thus be able to detect possible structural transitions associated to an energy change during pore filling. With this in mind, collecting thermodynamic data on various MOF/adsorbate systems in conjunction with molecular simulations may allow the building of a tool which will be able to predict whether a given probe molecule will induce this breathing effect. Molecular modeling based on classical force fields is most commonly used only to simulate adsorption isotherms without paying attention to the energetic nature of the adsorbate/adsorbent interactions which seems to be crucial in the breathing phenomenon occurring in MOF materials. The present work will show that the combination of X-ray powder diffraction (XRPD), simulations at the microscopic scale, and microcalorimetry is ideal to understand fully the onset of the flexibility in MOF materials upon the adsorption of different probe molecules.

MIL-53(Cr) or $\text{Cr}(\text{OH})(\text{O}_2\text{C}-\text{C}_6\text{H}_4-\text{CO}_2)$ is selected as a model system for its capability to either breathe or remain

unchanged upon adsorption, depending on the nature of the adsorbate molecules. Its structure is built up from infinite chains of corner-sharing $\text{CrO}_4(\text{OH})_2$ octahedra interconnected by terephthalate groups,²⁵ creating a 3D framework containing 1D diamond-shaped channels with pores of free diameter close to 8.5 Å in its large pore form. A number of studies have pointed out the flexibility of MIL-53(Cr) in the presence of carbon dioxide and water, corresponding to a structural switching between a large pore and a narrow pore form^{11,25–28} (Figure 1). On the other hand, this solid remains rigid upon adsorption of methane.⁷ Such a structure lends itself well to elucidating the flexibility of MOFs as both the large pore and narrow pore versions are structurally well defined, and the resulting structural switching can be simply followed by XRPD.

We selected a series of gases characterized by different intrinsic properties including apolar (Ar, hydrocarbons), polar (H_2O), and quadrupolar (N_2 , CO_2) molecules in order to generalize the origins of the flexibility in the MIL-53(Cr) system.

- (13) Horcajada, P.; Serre, C.; Vallet-Regi, M.; Sebban, M.; Taulelle, F.; Férey, G. *Angew. Chem., Int. Ed.* **2006**, *45*, 5974–5978.
- (14) Barthelet, K.; Marrot, J.; Riou, D.; Férey, G. *Angew. Chem., Int. Ed.* **2002**, *41*, 281–284.
- (15) Kitaura, R.; Fujimoto, K.; Noro, S. I.; Kondo, M.; Kitagawa, S. *Angew. Chem., Int. Ed.* **2002**, *41*, 133–135.
- (16) Fletcher, A. J.; Thomas, K. M.; Rossinsky, M. J. *J. Solid State Chem.* **2005**, *178*, 2491–2510.
- (17) Uemura, K.; Matsuda, R.; Kitagawa, S. *J. Solid State Chem.* **2005**, *178*, 2420–2429.
- (18) Kitagawa, S.; Uemura, K. *Chem. Soc. Rev.* **2005**, *34*, 109–119.
- (19) Takamizawa, S.; Nakata, E. I. *Cryst. Eng. Comm.* **2005**, *7*, 476479.
- (20) Matsuda, R.; Kitaura, R.; Kitagawa, S.; Kubota, Y.; Belosludov, R. V.; Kobayashi, T. C.; Sakamoto, H.; Chiba, T.; Takata, M.; Kawazoe, Y.; Mita, Y. *Nature* **2005**, *436*, 238–241.
- (21) Kubota, Y.; Takata, M.; Matsuda, R.; Kitaura, R.; Kitagawa, S.; Kobayashi, T. C. *Angew. Chem., Int. Ed.* **2006**, *45*, 4932–4936.
- (22) Kondo, A.; Noguchi, H.; Carlucci, L.; Proserpio, D. M.; Ciani, G.; Kajiro, H.; Ohba, T.; Kanoh, H.; Kaneko, K. *J. Am. Chem. Soc.* **2007**, *129*, 12362–12363.
- (23) Seki, K. *Phys. Chem. Chem. Phys.* **2002**, *4*, 1968–1971.
- (24) Serre, C.; Mellot-Draznieks, C.; Surble, S.; Audebrand, N.; Filinchuk, Y.; Férey, G. *Science* **2007**, *315*, 1828–1831.
- (25) Serre, C.; Millange, F.; Thouvenot, C.; Noguès, M.; Marsolier, G.; Louër, D.; Férey, G. *J. Am. Chem. Soc.* **2002**, *124*, 13519–13526.
- (26) Vimont, A.; Travert, A.; Bazin, P.; Lavalley, J.-C.; Daturi, M.; Serre, C.; Férey, G.; Bourrelly, S.; Llewellyn, P. L. *Chem. Commun.* **2007**, 3291–3293.
- (27) Ramsahye, N. A.; Maurin, G.; Bourrelly, S.; Llewellyn, P. L.; Loiseau, T.; Serre, C.; Férey, G. *Chem. Commun.* **2007**, 3261–3263.
- (28) Ramsahye, N. A.; Maurin, G.; Bourrelly, S.; Llewellyn, P.; Loiseau, T.; Férey, G. *Phys. Chem. Chem. Phys.* **2007**, *9*, 1059–1063.

Moreover, the use of C1 (methane) to C4 (*n*-butane) hydrocarbons allows a systematic increase of the probe size, without the introduction of functional chemical groups which would make these investigations more complex. Furthermore, both large and narrow pore forms of MIL-53(Cr) are easily modeled using computational assisted structural determination and Grand Canonical Monte Carlo simulations. This opens up the possibility to either compare or combine the experimental results with those obtained by computer simulations which will be used as a base to quantify the flexibility of MIL53(Cr) upon adsorption. In that way, it will allow us to define both energetic and steric criteria for inducing the breathing of this material.

Experimental and Computational Section

Synthesis. MIL-53(Cr) was synthesized using the published procedure,²⁵ and activation was performed in two steps: (i) exchange of the free terephthalic acid molecules filling the pores with DMF, and (ii) evacuation of DMF upon calcination.¹¹

Adsorption Microcalorimetry. The adsorption of hydrocarbons was carried out at 303 K using a manometric adsorption apparatus coupled with a Tian-Calvet type microcalorimeter.^{29,30} This experimental device measures the isotherm and the enthalpies of adsorption simultaneously using a point by point introduction of gas to the sample. Prior to each adsorption experiment, the samples were outgassed at 150 °C under a vacuum of 10^{-3} mbar. In these conditions, MIL-53(Cr) is present in its large pore form. The hydrocarbon gases were obtained from Air Liquide (Alphagaz, France). Each experiment was repeated several times, and both isotherms and enthalpy values were obtained by averaging over all the experiments.

Synchrotron XRPD. The in situ synchrotron powder diffraction experiments have been carried out at the Swiss-Norwegian Beamlines at the European Synchrotron Radiation Facility. The data were collected on the 0.7 mm quartz capillaries filled with the sample and attached to a gas manifold, using MAR345 imaging plate at a sample-to-detector distance of 250 mm, $\lambda = 0.71110$ Å. The data were integrated using Fit2D program (Dr. A. Hammersley, ESRF) and a calibration measurement of a NIST LaB₆ standard sample. The C1–C4 hydrocarbons (Alphagaz, France) were introduced at each pressure point. Equilibrium was assumed when two repeatedly measured diffraction patterns became identical.

X-Ray diagrams were indexed and refined by the Le Bail method using the DICVOL³¹ and FULLPROF³² softwares available in the WINPlotr suite.³³

Molecular Simulation. Molecular modeling has been used first to predict the structures of both the narrow and large pore forms in the presence of each type of hydrocarbon, starting with the cell parameters provided by the XRPD analysis (Tables 1 and 2). This structural determination was performed using energy minimization techniques allowing a full relaxation of all atomic coordinates and cell parameters. These simulations based on the UFF forcefield³⁴ were performed using Materials Studio softwares.³⁵ Once the frameworks of the MIL-53(Cr) were built, Grand Canonical Monte Carlo simulations based on validated force fields³⁶ to describe the

Table 1. Cell Parameters of the Narrow Pore Forms for MIL53(Cr) in the Presence of C1–C4 Hydrocarbons, Water, and Carbon Dioxide (Space Group *C2/c*)

gas	a (Å)	b (Å)	c (Å)	β (deg)	V (Å ³)	pressure (bar)
CH ₄	—	—	—	—	—	—
C ₂ H ₆	19.24(1)	9.89(1)	6.94(1)	107.52(1)	1258.7(1)	0.75
C ₃ H ₈	19.24(1)	10.08(1)	6.96(1)	109.12(1)	1275.6(1)	0.1
C ₄ H ₁₀	20.30(1)	10.60(1)	6.90(1)	112.55(1)	1370.8(1)	0.1
H ₂ O	19.68(1)	7.85(1)	6.78(1)	104.90(1)	1012.0(1)	0.005 ²⁵
CO ₂	19.71(1)	8.32(1)	6.80(1)	105.85(1)	1072.0(1)	1 ¹⁰

Table 2. Cell Parameters of the Large Pore Forms for MIL53(Cr) in the Presence of C1–C4 Hydrocarbons, Water, and Carbon Dioxide (Space Group *Imcm*)

gas	a (Å)	b (Å)	c (Å)	V (Å ³)	pressure (bar)
—	16.733(1)	13.038(1)	6.812(1)	1486.1(1)	0 ²⁰
CH ₄	16.444(1)	13.512(1)	6.834(1)	1518.6(1)	33
C ₂ H ₆	16.109(1)	13.938(1)	6.836(1)	1535.0(1)	13.5
C ₃ H ₈	16.190(1)	13.820(1)	6.835(1)	1529.4(1)	10
C ₄ H ₁₀	16.103(1)	13.925(1)	6.833(1)	1532.4(1)	0.5
H ₂ O	16.733(1)	13.038(1)	6.812(1)	1486.1(1)	—
CO ₂	16.439(1)	13.500(1)	6.831(1)	1516.0(1)	16

interactions between the hydrocarbons and the MIL framework were performed at 303 K with a simulation box corresponding to 16 unit cells with typically 3×10^6 Monte Carlo steps. The adsorption enthalpy at low coverage was calculated in both narrow and large pore forms for each C1–C4 hydrocarbon, through the fluctuation over the number of particles in the system and from the internal energy.³⁷ It has to be mentioned that, in a first approximation, the narrow pore structure in the presence of C2 was also considered for C1 in order to provide a hypothetical value of the enthalpy of adsorption, if MIL-53(Cr) would breathe. Both electrostatic and short-range interactions have been estimated using a cutoff distance of 12 Å, and an additional Ewald summation has been used to calculate the electrostatic terms.

Results and Discussion

In an initial series of experiments, the isotherms and enthalpies of adsorption of the four hydrocarbons were measured at 303 K. The isotherms given in Figure 2a, are of Langmuir type when reported in a standard form as amount adsorbed (as $\text{cm}^3_{\text{liq}} \text{g}^{-1}$) versus pressure. However, when plotted as a function of the log of the pressure (Figure 2b), one can distinguish a step in the C3 and C4 isotherms while a convex shape is obtained for the C2 adsorption. By contrast, only a concave profile is pointed out for C1 which is commonly observed when plotting a Langmuir isotherm for a rigid microporous material. The steps in the C3 and C4 isotherms may be the signature of the breathing of the MIL-53(Cr) structure upon adsorption as was previously observed for carbon dioxide.^{7,11} The convex profile observed for C2 may be assigned to an intermediate behavior between the two types of isotherms. Furthermore, while the amounts adsorbed in terms of liquid volume increase from methane to propane, the opposite trend is observed in terms of number of molecules per unit cell. It is of interest to use both scales as this shows the complementarity between macroscopic (liquid volume) and microscopic (number of molecules per unit cell) representations of the adsorption data. Indeed, both representa-

(29) Llewellyn, P. L.; Maurin, G. C. R. *Chimie* **2005**, *8*, 283–302.

(30) Llewellyn, P. L.; Maurin, G. Gas adsorption in zeolites and related materials. In *Introduction to zeolite molecular sieves*; van Bekkum, H.; Cejka, J.; Corma, A.; Schüth, F. Eds.; Elsevier: Amsterdam, 2007, pp 555–610.

(31) Altomare, A.; Caliandro, R.; Camalli, M.; Cuocci, C.; Giacovazzo, C.; Moliterni, A. G. G.; Rizzi, R. *J. Appl. Crystallogr.* **2004**, *37*, 1025–1028.

(32) Rodriguez-Carvajal, J. Fullprof Suite, LLB Sacley & LCSIM Rennes, France, 2005.

(33) Roisnel, T.; Rodriguez-Carvajal, J. *J. Mater. Sci. Forum* **2001**, *378–381*, 118–123.

(34) Rappé, A. K.; Casewit, C. J.; Colwell, S.; Goddard, W. A., III; Skiff, W. M. *J. Am. Chem. Soc.* **1992**, *114*, 10024.

(35) Accelrys, 4.2 ed.; San Diego, CA, and Cambridge, U.K.

(36) Rosenbach, N.; Jobic, H.; Salles, F.; Maurin, G.; Bourrelly, S.; Llewellyn, P. L.; Devic, T.; Serre, C.; Férey, G. *Angew. Chem.* **2008**, *120*, 6713–6717.

(37) Nicholson, D.; Parsonage, N. G. *Computer simulation and the statistical mechanics of adsorption*; Academic Press: London, 1982.

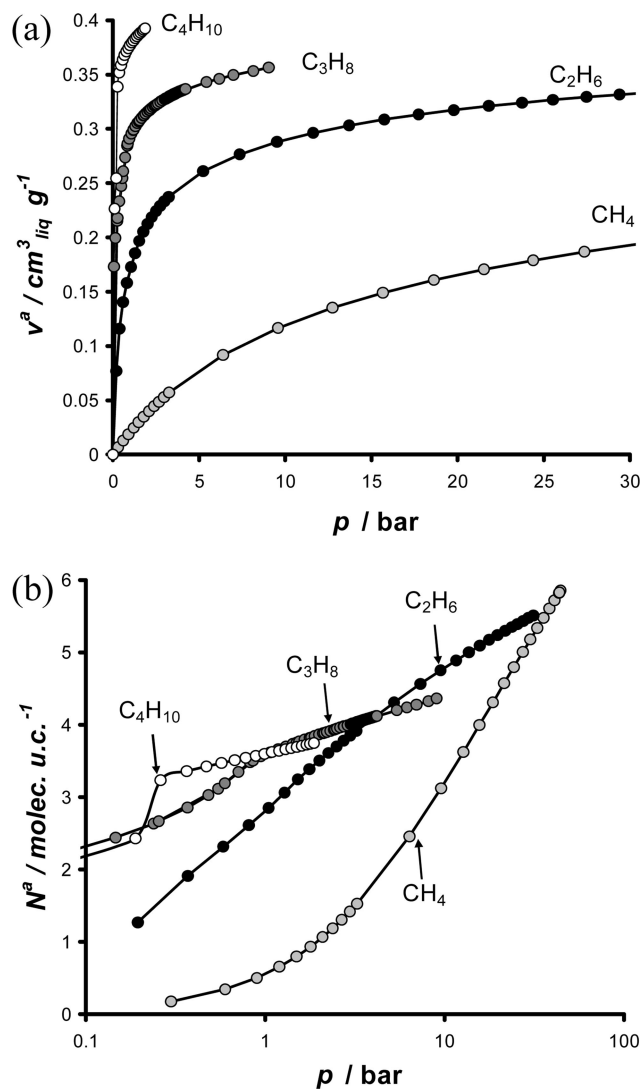


Figure 2. Isotherms (a) standard and (b) semilog scale) obtained at 303K during the adsorption of the C1–C4 hydrocarbons on MIL-53(Cr).

tions are of interest with respect either to applications or when one aims to get a microscopic picture of the adsorption process.

However, at this stage, no conclusive information on the structural behavior of the MIL-53(Cr) solid during the adsorption can be extracted. To go further, in situ XRPD patterns were collected during the hydrocarbon adsorption using a specific adsorption apparatus developed for experiments at the Swiss-Norwegian beamline at the ESRF. The patterns thus obtained can initially be compared to those previously obtained in the case of carbon dioxide adsorption (schematized in Figure 1). An indexing and refinement of these peaks is given in Tables 1 and 2.

All the X-ray diffraction patterns (Figure 3) show that the initial adsorption of gas occurs in the outgassed, large pore form of MIL53(Cr) (as also schematized in Figure 1). In the case of methane, this large pore form is observed at all methane pressures, even up to 33 bar. A different behavior is observed in the case of the C2–C4 hydrocarbons. The initial large pore form is present at low pressures before the observation of a two-phase region corresponding to the coexistence of the large and the narrow pore forms. It can be seen that the proportion of the narrow pore form with respect to the large pore form increases from ethane to butane (Figure 3). This coexistence of

phases occurs to some proportion in all of the adsorption systems studied so far in MIL53(Cr). This has even been the case, to a small extent, with CO_2 and H_2O . This phase coexistence seems more pronounced in the case of the hydrocarbons as the pressure range of stability of the narrow pore phase is relatively small. The only tentative explanation that can be given at the present time is that the energy difference between the open and narrow pore systems with loaded gas depends on the nature of this gas from both an energetic and entropic point of view.

XRPD shows unambiguously the evolution of the flexible character of the MIL-53(Cr) structure with the hydrocarbon chain length. Once the peaks corresponding to the large and narrow forms were identified, their cell parameters were refined (Tables 1 and 2). The unit cell volume of the narrow pore version increases from 1258.7(1) to 1275.6(1) to 1370.8(1) \AA^3 for ethane, propane, and butane, respectively, in relation with steric effects. The size of hydrocarbon molecules significantly limits the degree of contraction when compared with smaller sorbates such as carbon dioxide ($V = 1072 \text{ \AA}^3$ ¹⁰) and water ($V = 1012 \text{ \AA}^3$ ²⁵). The reopening of the structure at higher pressure unambiguously shows the presence of the only large pore version (Figure 3) with assigned volumes only slightly higher than those observed for the outgassed structure (Table 2). This large \rightarrow narrow \rightarrow large pore transition with gas filling has been termed ‘breathing’ in the case of carbon dioxide.¹¹ The difference observed here in the case of the hydrocarbons is that the narrow pore form is present only in a tiny region of pressure.

Our previous work focused on the adsorption of carbon dioxide in MIL-53(Cr) has shown that the flexibility of this MOF upon adsorption of probe molecules is usually accompanied by a distinct variation in the adsorption enthalpy.^{7,11} The possibility to directly follow the evolution of the enthalpy during the whole adsorption process is thus a key point to understand why these materials either undergo or do not undergo such breathing phenomena. The enthalpies of adsorption for methane were previously reported and show a slight increase with increasing loading.⁷ This trend is usually interpreted as an interaction between the gas and a homogeneous energetic surface, the slight increase in enthalpy with the loading being mainly due to an increase of the methane–methane interactions. Here, in the low domain of pressure for C2–C4 hydrocarbons, the enthalpies increase up to a maximum and then slightly decrease with pressure (Figure S1). This behavior was previously observed for carbon dioxide.^{7,11} Here, the initial enthalpy values observed for all hydrocarbons are due to the adsorption in the large pore outgassed form of MIL-53(Cr). Further, the maximum value in the enthalpies corresponds to a pressure at which the narrow pore structure starts to appear in the XRPD patterns (Figure 3). This observation is not so surprising as an increase in molecular confinement results in an enhanced interaction of the probe molecule with the pore wall.

To verify this assumption, a direct comparison with molecular simulation is of great interest. In that way, Grand Canonical Monte Carlo simulations were performed to estimate the enthalpy of adsorption resulting from the adsorption of the first molecule for each C1–C4 hydrocarbon in both the narrow and large pore forms (Figure 4). For the C2–C4 hydrocarbons, a good agreement is again observed for the measured enthalpies at the initial loading and the simulated values for the large pore form of MIL-53(Cr). Further, it is also interesting to note that very similar simulated enthalpies are obtained for methane in both large pore and narrow pore forms, which compare well

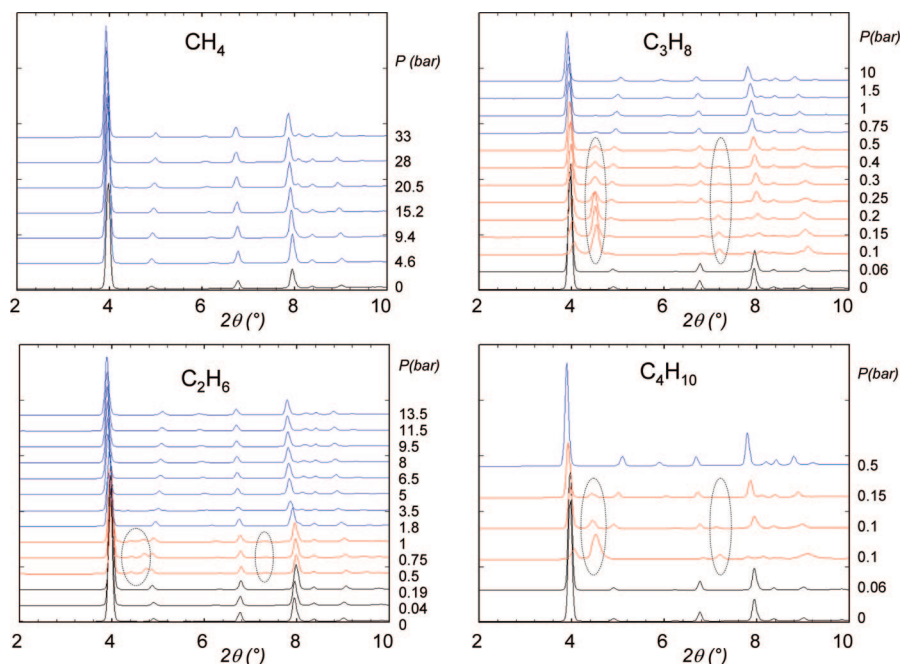


Figure 3. Variation of the XRPD patterns of MIL-53(Cr) with the alkane pressure at 303 K ($\lambda = 0.71110 \text{ \AA}$). Black: large pore form (empty pores). Red: mixture of narrow and large pore form. Blue: large pore form (pores filled). Main peaks belonging to the narrow pore form are highlighted.

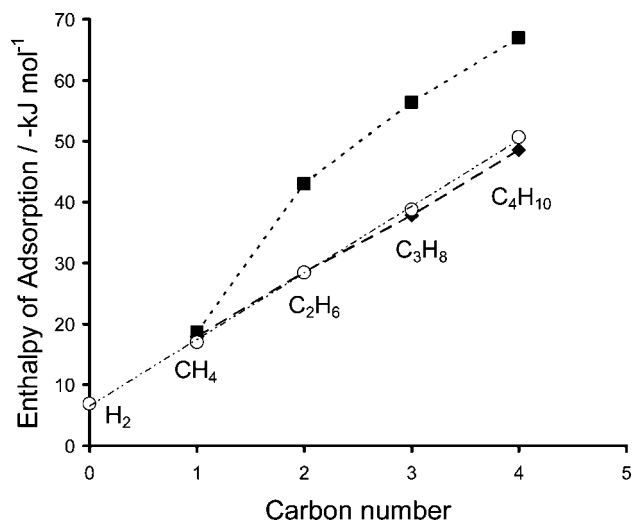


Figure 4. Enthalpies of adsorption obtained by Grand Canonical Monte Carlo simulations on the large (black diamonds) and narrow pore (black squares) forms of MIL-53(Cr) and by microcalorimetry at the initial loading (open circles). Experimental error $\pm 0.5 \text{ kJ mol}^{-1}$.

with the average value obtained by microcalorimetry. For the narrow pore form, we only report the simulated data as the coexistence of the large and narrow pore forms in the intermediate pressure range does not allow us to attribute rigorously an experimental value to that form. This clearly establishes that an increase in carbon chain length leads to an almost linear incremental increase in enthalpy of adsorption for both large and narrow pore forms. Such a behavior is similar to that observed for the adsorption of hydrocarbons in small pore zeolites.^{38,39} It thus seems possible to predict the interaction energies for longer chain lengths.

The data from microcalorimetry can be a starting point to elucidate which are the thermodynamic criteria for an adsorbed molecule to induce the flexibility of the MIL-53(Cr) structure. Indeed, a certain minimum energy is required for initiating this structural transition. This could correspond to the initial enthalpy of adsorption when the gas starts to be adsorbed in the large pore form of the material. This adsorption energy would thus drive the structural switching from the large to the narrow pore forms. As a consequence, each adsorbate giving rise to an adsorption enthalpy in the large pore form higher than this energy threshold would induce the breathing effect. If this energetic condition would not be satisfied, the structure would remain open in the large pore form. This thermodynamic criterion is supported by several examples of experimental evidence: the adsorption of argon, oxygen, and nitrogen does not induce any flexibility in the MIL-53(Cr), and the initial enthalpies of adsorption are of around -14 to -15 kJ mol^{-1} for these three gases (Figure S2). The observed value for CH_4 (-18 kJ mol^{-1}) leads to the large pore form in the whole range of pressure. By contrast, the enthalpy of adsorption in the large pore form for CO_2 of about -21 kJ mol^{-1} induces the breathing of the MIL framework.^{7,11,27} These data suggest that there is very little tolerance on the energetic criterion to induce the structural switching, and that a value of $\approx 20 \text{ kJ mol}^{-1}$ would be required to induce the contraction of MIL-53(Cr). The initial enthalpies of -28.5 , -38.8 , and $-50.7 \text{ kJ mol}^{-1}$ for ethane, propane, and butane then allow the adsorbent flexibility. In the same way, water adsorption occurs with an initial value of -53 kJ mol^{-1} , and again the flexibility is observed.

Turning to the reopening of the MIL-53(Cr) structure at higher pressure, it is possible to relate this transition to the enthalpy of adsorption in the narrow pore form via a semilog relationship (Figure 5). For that purpose, experimental and simulated enthalpies are also reported for water and carbon dioxide and

(38) Denayer, J. F. M.; De Meyer, K.; Martens, J. A.; Baron, G. V. *Angew. Chem., Int. Ed.* **2003**, *42*, 2774–2777.

(39) Denayer, J. F. M.; Ocakoglu, R. A.; Arik, I. C.; Kirschhock, C. E. A.; Martens, J. A.; Baron, G. V. *Angew. Chem., Int. Ed.* **2005**, *44*, 400–403.

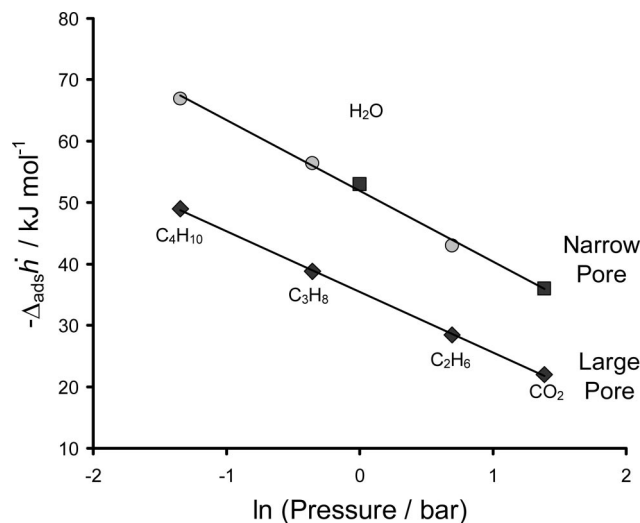


Figure 5. Enthalpies of adsorption as a function of $\ln(p)$ where p corresponds to the pressure range of the ‘narrow–large’ pore transition for carbon dioxide, water, and the C₂–C₄ hydrocarbons determined from the isotherms. Diamonds: initial enthalpies measured in the large pore form of MIL53(Cr). Squares: enthalpy measured during the filling of the narrow pore. Circles: simulated enthalpies for narrow pore filling.

the C₂–C₄ hydrocarbons. An almost linear relationship is obtained when one considers the enthalpy of adsorption for the narrow pore forms. Such a correlation is also obtained taking into account the enthalpy at the initial stage of adsorption in the large pore form as highlighted in Figure 5.

The fact that a straight line relationship is found is not so surprising as many expressions relate the gas–solid interaction to $\ln(p)$. One can use such a relationship for this sample to predict the pressure of reopening not only from the enthalpy of the narrow pore form but also from the initial enthalpy of adsorption measured in the large pore version of MIL-53(Cr). What is of interest here is that the higher the enthalpy of adsorption, the lower the transition pressure from the narrow pore to large pore. It has been suggested for stable states of flexible MOFs that the difference in equilibrium energy between each state should be much greater than kT .⁴⁰ Thus the higher the enthalpy of adsorption, the easier it is for the framework to get the minimum energy required for the narrow to large pore structure transition which is known to be endothermic. Furthermore, the isotherms in the present study suggest that a certain quantity of adsorbed molecules is required for the reopening of the structure and this ‘critical amount adsorbed’ is attained at lower pressures for the longer chain hydrocarbons than for carbon dioxide for example. This would suggest that the energy of the adsorbate/adsorbate interactions also play an important role in the structural switching.

Interestingly, the linear relation obtained from the adsorption enthalpy at the initial stage of loading would suggest that the pressure required for the reopening of the MIL-53(Cr) can be predicted only from the knowledge of the strength of the interactions in the outgassed material.

The thermodynamic treatment given above enables the prediction of whether breathing will occur and at which pressure. Further information can be gained from a structural standpoint. One can define a ‘magnitude of breathing’, which can be taken as the percentage difference in cell volumes between the narrow

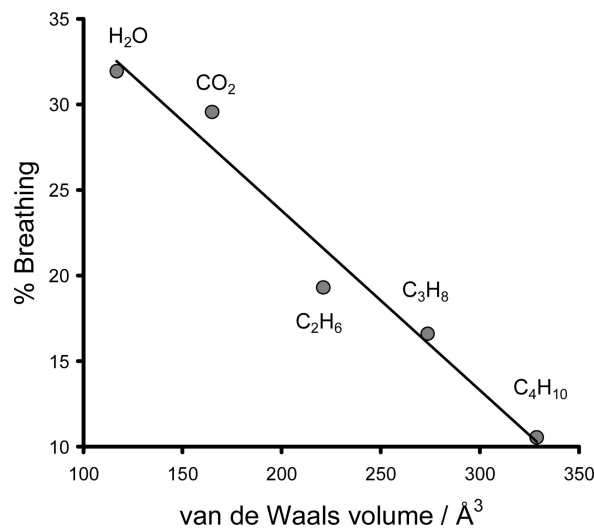


Figure 6. Variation of percent breathing as a function of the probe molecule van der Waals volume.

and large pores with respect to the initial cell volume of the large pore (i.e., $(V_{\text{large pore}} - V_{\text{narrow pore}})/V_{\text{large pore}}$). Figure 6 shows that this amplitude of breathing can be related to the dimensions of the probe molecule, in the form of its van der Waals volume. The straight line relationship shown here suggests that the smaller the molecule, the larger the amplitude that the MIL53(Cr) structure is able to breathe. This observation clearly emphasizes how MOF frameworks in general can accommodate their pore closing/opening depending on the nature of the guest molecules.

Conclusions

This investigation attempts to further understand and predict MOF breathing. MIL-53(Cr) has been selected as a model system, as this structure exists in two well-defined states. Initially the sample is in the large pore form, and depending on the fluid, a shrinkage of the structure occurs prior to a reopening at higher pressure. This work suggests that a minimum energy is required for this first ‘large to narrow’ pore transition to occur and that a minimum pressure is then required to induce the following ‘narrow–large’ pore transition. It would seem that the value of the enthalpy of adsorption governs whether a structural transition occurs, and in the case here, we suggest that a minimum enthalpy in the initial large pore form of around -20 kJ mol^{-1} is required to contract the system. More interestingly, the knowledge of the adsorption enthalpy in the large pore form can further be used to predict the pressure of the reopening of the structure via a simple semilog relationship which holds for the nonpolar hydrocarbons as well as for carbon dioxide and water. It is thus shown that higher the enthalpy, the lower the transition pressure from the narrow pore to large pore. Finally, from the molecular size of the adsorbate, it is possible to estimate the degree of contraction of the pore structure showing that the MIL framework is able to adapt its pore closing/opening depending on the nature of the guest molecules. This original property makes this material promising as a potential nanovector for drug delivery where an optimization of the drug/matrix interaction is required.

We have shown that the thermodynamic information that can be directly obtained experimentally using microcalorimetry, when combined with molecular simulation, is essential to understand and predict the onset of flexibility in this structure upon the adsorption of probe molecules and also the approximate

(40) Zhang, J.-P.; Chen, X.-M. *J. Am. Chem. Soc.* **2008**, *130* (18), 6010–6017.

pressure required to reopen the system. These conclusions could be extended to the flexibility of other MOF systems.

Acknowledgment. The authors acknowledge the financial support of the French ANR 'SAFHS' (ANR-07-BLAN-0284-02). S.L.-S. and N.R. are indebted for the support of the European Alfa program 'NANOGASTOR' (II-0493-FA-FI). We are grateful to the ESRF for providing access to the Swiss-Norwegian beamline.

Supporting Information Available: The differential enthalpies of adsorption, given in this Supporting Information, are those at low pressure for the C1–C4 hydrocarbons (Figure S1) and for N₂, Ar and O₂ (Figure S2). This material is available free of charge via the Internet at <http://pubs.acs.org>.

JA803899Q